Interactions of very long-chain saturated fatty acids with serum albumin

Ji-Kyung Choi,* Jet Ho,* Stephen Curry,† Donghui Qin,§ Robert Bittman,§ and James A. Hamilton[1,*]

Department of Physiology and Biophysics,* Boston University School of Medicine, 715 Albany Street, Boston, MA 02118; Biophysics Section,† Blackett Laboratory, Imperial College of Science, Technology, and Medicine, London SW7 2BW United Kingdom; and the Department of Chemistry and Biochemistry,§ Queens College of the City University of New York, Flushing, NY 11367

Abstract The remarkable binding properties of serum albumin have been investigated extensively, but little is known about an important class of fatty acids, the very long-chain saturated fatty acids (VLCFA; >18 carbons). Although VLCFA are metabolized efficiently in normal individuals, they are markers for and possibly causative agents of several peroxisomal disorders. We studied the binding of [^{13}C]carboxyl-enriched arachidic (C20:0), behenic (C22:0), lignoceric (C24:0), and hexacosanoic (C26:0) acids to bovine serum albumin (BSA) by ^{13}C-NMR spectroscopy. For each VLCFA, the NMR spectra showed multiple signals at chemical shifts previously identified for long-chain fatty acids (12–18 carbons), suggesting stabilization of binding by similar, if not identical, interactions of the fatty acid carboxyl anion with basic amino acid residues. The maximal binding (mol of VLCFA/mol of BSA) and the number of observed binding sites decreased with increasing chain length, from 4–5 for C20:0, 3–4 for C22:0, and 2 for C24:0; we validated our previous conclusion that BSA has only one site for C26:0 (Ho, J. K., H. Moser, Y. Kishimoto, and J. A. Hamilton. 1995. *J. Clin. Invest.* 96: 1455–1463). Analysis of chemical shifts suggested that the highest affinity sites for VLCFA are low affinity sites for long-chain fatty acids. In competition experiments with ^{13}C-labeled C22:0 (3 mol/mol of BSA) and unlabeled oleic acid, C22:0 bound to BSA in the presence of up to 4 mol of oleic acid/mol of BSA, but 1 mol was shifted into a different site. Our studies suggest that albumin has adequate binding capacity for the low plasma levels of VLCFA with 20 to 26 carbons, but the protein may not be able to bind longer chain VLCFA.—Choi, J-K., J. Ho, S. Curry, D. Qin, R. Bittman, and J. A. Hamilton. **Interactions of very long-chain saturated fatty acids with BSA. *J. Lipid Res.* 2002.** 43: **1000–1010.**

Supplementary key words fatty acid transport • lipid-protein interactions • ^{13}C-NMR spectroscopy • adrenoleukodystrophy

Serum albumin is a remarkable protein capable of binding numerous ligands (1–4). Most of the naturally occurring ligands are hydrophobic and poorly soluble in a purely aqueous medium (1, 4). Albumin is also an extremely unusual protein in having multiple high-affinity binding sites for the same ligand, unesterified fatty acid (1, 5). Saturated fatty acids bind with increasing affinity as their chain length increases, at least between chain lengths of eight (octanoic) and 18 (stearic) carbons, possibly because of an increase in hydrophobic interactions (5). However, binding to albumin appears to diminish when a chain length of 20 carbons is reached (6). Because very long-chain saturated fatty acids (VLCFA; acyl chain >18 carbons) are so insoluble in water, both the delivery of fatty acids to albumin and the measurement of the unbound aqueous pool of fatty acids are difficult, which hampers classical binding studies (6).

Our laboratory developed an NMR spectroscopic approach to investigate the binding interactions of fatty acids with various lipid-binding proteins, such as serum albumin and intracellular fatty acid-binding proteins (7–10). This approach uses [^{13}C]carboxyl-enriched fatty acids to enhance the sensitivity of ^{13}C-NMR spectroscopy to detect subtle differences in the microenvironment of the carboxyl upon binding. For BSA, these studies have revealed the number of binding sites, the filling of individual binding sites, the modes of interactions of fatty acids with nearby amino acids, the ionization behavior of the fatty acid in individual binding sites, and the general locations of the high-affinity sites of long-chain fatty acids (11–14).

Recent crystallographic structures of complexes of human serum albumin (HSA) with saturated fatty acids with

Manuscript received 23 January 2002 and in revised form 14 April 2002.
DOI 10.1194/jlr.M200041-JLR200

Abbreviations: HSA, human serum albumin; Ms, methanesulfonyl; PC, phosphatidylcholine; SUV, small unilamellar vesicles; VLCFA, very long-chain fatty acids.

[1] To whom correspondence should be addressed.
e-mail: jhamilt@bu.edu

10 to 18 carbons have revealed precise locations and molecular interactions of up to 11 fatty acid molecules (15). The X-ray structure validated several predictions from [^{13}C]NMR studies, including the presence of salt bridges between the fatty acid carboxyl and basic amino acid residues in most binding sites and the general localization of the fatty acid in the different domains of albumin (16, 17). The crystal structure with spatially distinct binding sites is consistent with the NMR finding of slow exchange (on the chemical-shift time scale) of long-chain fatty acids between binding sites (10).

The present study investigates the interaction of BSA with four VLCFA, for which there is little or no binding information. Although less abundant than the long-chain fatty acids, VLCFA are normally synthesized and metabolized in the body (18). The importance of VLCFA in normal human physiology is emphasized by the recent discovery of a family of proteins involved in their metabolism. Originally proposed to function as transporters for the translocation of fatty acids across the plasma membrane of cells, and called FATP (fatty acid transport protein) (19), three of the six proteins in this family have now been shown to have acyl CoA synthetase activity toward VLCFA (20–22).

Certain VLCFA (e.g., C24:0 and C26:0) are chemical markers of peroxisomal disorders of fatty acid metabolism, such as adrenoleukodystrophy, in which saturated VLCFA accumulate to high levels in patients' tissues and plasma. VLCFA may also be a causative factor of these disorders (23–25). In our NMR assay, the 26-carbon hexacosanoic acid showed very limited binding to albumin; we observed only one binding site with a capacity of one fatty acid molecule (26). Therefore, for VLCFA containing 20, 22, and 24 carbons, there is either a progressive decrease or a sharp cutoff in binding capacity. In the present study we systematically investigated the binding interactions of VLCFA of different chain lengths (C20:0, C22:0, C24:0, C26:0) by [^{13}C]NMR spectroscopy, monitored the appearance of higher- and lower-affinity sites, and determined the maximal binding capacity for each VLCFA.

MATERIALS AND METHODS

Materials

Egg yolk phosphatidylcholine (PC) was purchased from Avanti Polar Lipids (Alabaster, AL) and used without further purification; essentially fatty acid-free BSA (fraction V) was purchased from Sigma (St. Louis, MO); 80% [1-^{13}C]arachidic acid (C20:0) was obtained from Cambridge Isotope Laboratories (Andover, MA). Silica gel TLC plates (25 μm thickness) were used to monitor the reactions, with visualization by charring using 10% H_2SO_4 in ethanol. Flash chromatography was carried out on silica gel 60 (230–400 ASTM mesh) of E. Merck, purchased from Sigma-Aldrich.

Synthesis of [^{13}C]carboxyl-enriched VLCFA

[^{13}C]carboxyl-enriched VLCFA [behenic acid (C22:0), lignoceric acid (C24:0), and hexacosanoic acid (C26:0)] were synthesized by modification of a previous procedure (26) with a purity of 99%, 97%, and 100%, respectively, with the indicated yields (Eqs. 1–3).

$$CH_3(CH_2)_nOH \xrightarrow[0°C-rt,\ 3\ h]{MsCl/py} CH_3(CH_2)_nOMs \quad (Eq.\ 1)$$

$$n = 19,21,23 \qquad (90-95\%)$$

$$CH_3(CH_2)_nOMs \xrightarrow[C_6H_6,\ reflux,12\ h]{CH_2(^{13}CO_2Et)_2/NaH} CH_3(CH_2)_nCH(^{13}CO_2Et)_2 \quad (Eq.\ 2)$$

$$(74-76\%)$$

$$CH_3(CH_2)_nCH(^{13}CO_2Et)_2 \xrightarrow[reflux,\ 3\ days]{conc.\ HCl} CH_3(CH_2)_{n+1}{}^{13}CO_2H + {}^{13}CO_2 \quad (Eq.\ 3)$$

$$(74-90\%)$$

The modifications were as follows: first, in Eq. 2, the malonate was used as the limiting reagent rather than the alkyl mesylate; the latter was prepared as shown in Eq. 1. Second, both the esterification and decarboxylation reactions were carried out in the same pot by heating the diethyl 2-*n*-alkyl-[1,3-$^{13}C_2$]malonate (1.1 mmol) in 20 ml of concentrated HCl at 120°C (oil bath temperature) for 3 days (Eq. 3).

Preparation of BSA solutions

BSA was weighed and dissolved in 0.8 ml of 50 mM phosphate buffer (pH = 7.4) and 0.2 ml D_2O. The concentration of the BSA solution was determined by measuring optical density at 280 nm with a Perkin-Elmer Lambda 2 UV/VIS spectrometer. The final concentration of BSA for direct binding studies was 50 mg/ml, and 100 mg/ml for studies in which albumin was added to vesicles.

Preparation of VLCFA for delivery to BSA: K^+ salts and VLCFA/phospholipid vesicles

The crystalline VLCFA was dissolved in $CHCl_3$ and the concentration of each VLCFA determined by dry weight measurements on a Cahn Electro balance. For C20:0 and C22:0, stock solutions of the K^+ salt were prepared by a method similar to that previously used for long chain fatty acids (11, 12). A measured amount of the $CHCl_3$ solution of the VLCFA was dried under N_2 and lyophilized to give a powder that is easier to disperse than the original crystalline VLCFA. KOH equivalents of 1.2 (relative to the fatty acid) in a known volume of H_2O were added. The VLCFA dissolved to make a clear solution after shaking on a vortex mixer and heating in a hot water bath. Unless used immediately, this stock solution became turbid at room temperature, and prior to addition to BSA, the solution was warmed again to achieve dissolution and homogeneity.

The solubility in aqueous solution of VLCFA with ⩾24 carbons was too low to permit preparation of the potassium salt at the desired concentration. In this case, the VLCFA was incorporated into small unilamellar vesicles (SUV) to disperse or solubilize the VLCFA according to the following procedure. The concentration of PC in chloroform was determined from its dry weight, and the desired amount of C24:0 or C26:0 in $CHCl_3$ was added. After chloroform was evaporated under a stream of N_2, the sample was lyophilized overnight for complete removal of solvent. The PC/VLCFA mixture was hydrated with 0.7 ml of 50 mM pH 7.4-phosphate buffer and 0.3 ml of D_2O. Later, 0.5 ml of phosphate buffer was used to wash the vial. The sample was then sonicated for 1 h with a Sonifier cell disrupter 350 equipped with a Branson microtip. The resultant SUV preparation was centrifuged for 30 min to remove fragments of the sonifier tip. The same procedure was used to prepare SUV with C22:0 as a control experiment. The final composition of the vesicles (VLCFA/phospholipid) was assumed to reflect the initial composition.

Preparation of fatty acid/BSA complexes

To make complexes of C20:0 or C22:0 with BSA, the desired aliquot of VLCFA was added to a known volume and concentration of BSA, prepared as above, in a water bath at 37 C. The vol-

ume of each aliquot was chosen to give one mole of VLCFA/mole of BSA. For NMR experiments monitoring the filling of binding sites, each sample was prepared by the incremental addition of 1 mol of C20:0 or C22:0 to minimize artifacts from the precipitation of VLCFA.

To study binding of C24:0 and C26:0 to BSA, the VLCFA was delivered to BSA by incubation of a known volume of vesicles containing C24:0 or C26:0 with the desired amount of aqueous BSA, as described previously for C26:0 (26). To relate the results of the two approaches for loading VLCFA onto BSA, vesicles with C22:0 were prepared and studied in a parallel experiment.

NMR spectroscopy

NMR spectra were obtained on a Bruker DMX-500 spectrometer equipped with a 10 mm broadband probe. Samples (2 ml with 15% D_2O for a lock signal) were maintained at 38°C. ^{13}C-NMR spectra were acquired with 3 s pulse intervals and broadband ^{1}H decoupling. The chemical shift of the ε-Lys/β-Leu carbons (δ = 39.57 ppm) from the albumin was used as an internal reference (10).

Modeling of the binding of C26:0 to albumin

Human serum albumin (HSA) was used as a model for BSA since the structure of BSA has not been determined. However, the two proteins share 75% sequence identity and are thus likely to have very similar structures. In the HSA structure, medium and long-chain fatty acids bind in similar configurations in seven binding sites (15). In five of these sites (numbered 1–5 in Fig. 8), the side chains of conserved amino acids make salt bridges with the bound fatty acid, essentially locking the carboxyl in place. Using the structure of HAS-18:0 (PDB ID 1e7i) as a template, we modeled bound configurations of C26:0 into these five sites. In each case, we superposed the carboxylate moieties of C18:0 and C26:0 and endeavored to fit the methylene tail into the hydrophobic portion of the pocket with reasonable stereochemistry. All manipulations were performed using the program O (27).

RESULTS

Direct binding studies of C18:1, C20:0, and C22:0

The binding of oleic acid to BSA, as visualized by ^{13}C-NMR spectra of the fatty acid carboxyl carbon, is very similar to that of palmitic acid and stearic acid (12). Although spectra of oleic acid/BSA complexes have been analyzed in detail at a lower magnetic field (4.73 T) (10), new spectra were attained at a higher field (11.75 T) with enhanced resolution for comparison with spectra of VLCFA. The carbonyl region of the ^{13}C spectrum of BSA with no added fatty acid (**Fig. 1A**) contains a broad peak at 170 to 180 ppm representing carbonyl groups from the protein peptide backbone and some side-chain carboxyl

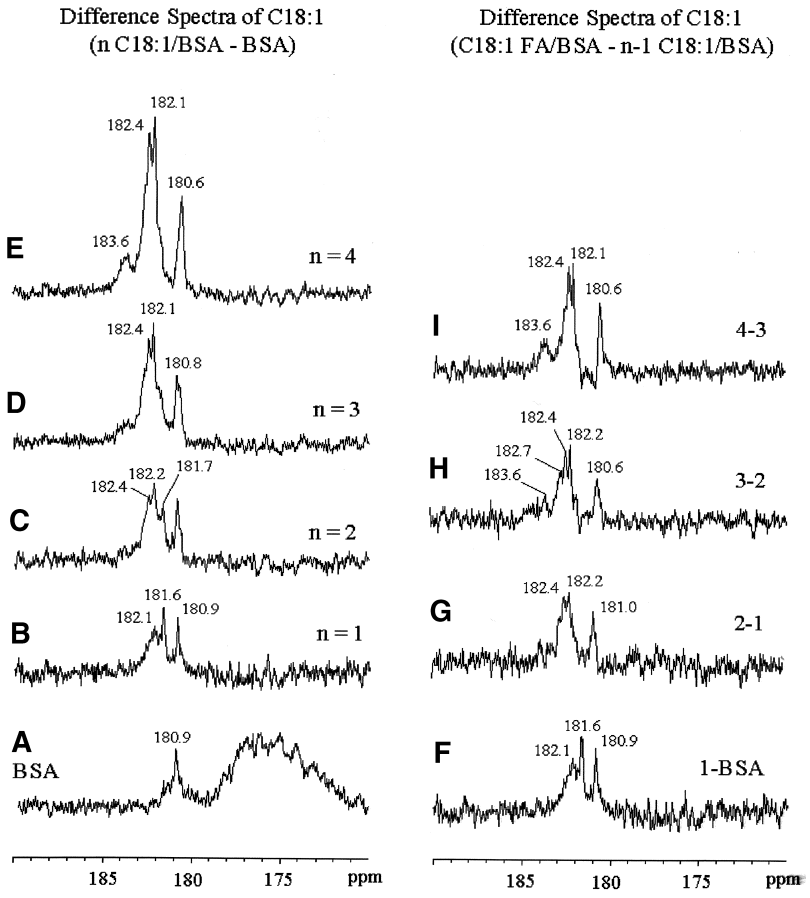

Fig. 1. Carboxyl and carbonyl region (170–190 ppm) of the ^{13}C-NMR spectra of oleic acid bound to BSA between 1 and 4 mol C18:1/mol BSA after 2,400 spectral accumulations. A–E: The contribution of BSA was subtracted digitally in B–E. F–I: Difference spectra of (N+1) C18:1/BSA–N C18:1/BSA. All spectra were acquired at 38°C with a 2.0 s pulse interval and 32,000 time-domain points.

groups, and a narrow peak at 180.9 from glutamate carboxyl groups (10).

The spectra of oleic acid/BSA complexes (Fig. 1B–E) are presented after subtraction of the spectrum of fatty acid-free BSA obtained under the same spectrometer conditions (Fig. 1A) to remove the contribution of protein resonances. The narrow carboxyl peaks represent ^{13}C-labeled oleic acid in binding sites on the albumin molecule. The three peaks at 182.4 ppm, 182.1–182.2 ppm, and 180.6–180.9 ppm (Fig. 1) were previously designated as "b, c, and d" and represent three primary binding sites for oleic acid (10). In addition, a signal at 181.6 ppm was detected at the lowest fatty acid-BSA ratio studied (fatty acid-BSA = 1.0); this was not clearly seen in previous spectra with lower signal-to-noise ratios. Although the peak is relatively intense at 1 mol of oleic acid, it becomes less significant at higher mol ratios, as shown by the difference spectra (Fig. 1F–I). Consistent with previous studies, an additional peak at 183.6 ppm (peak "a" in ref. 10) is initially very week and becomes more detectable at 3–4 mol oleic acid/BSA. Above 4 mol oleic acid/BSA, ^{13}C-NMR spectra show a continuous increase in the total fatty acid carboxyl signal up to a ratio of 8 to 10 mol, at which fatty acids begins to precipitate as an acid-soap (11, 12).

The spectra of the C20:0/BSA complex (**Fig. 2**) show multiple signals from the bound fatty acid as for oleic acid/BSA complexes (Fig. 1). Spectra at the higher mol ratios for these two fatty acids are generally similar, but the filling of binding sites is very distinct. At a 1:1 mol ratio of C20:0-BSA (Fig. 2A), there are only two significant peaks for C20:0 (182.5 and 182.7 ppm), both at higher ppm compared with the signals from oleic acid at the same fatty acid-BSA ratio (Fig. 1B). In addition, the prominent peak for oleic acid at ~181.0 ppm is barely visible for C20:0. However, a peak at this position increases in intensity as the C20:0-BSA ratio increases (Fig. 2A–D). At 3 mol of C20:0/BSA, there are three strong signals (180.9, 182.2–182.4, and 182.7 ppm); except for the peak at 182.7 ppm (Fig. 2C), these peaks appear at approximately the chemical shifts as the most intense signals (180.8, 182.2, 182.4 ppm) of oleic acid (Fig. 1C). There is a very small increase in the total intensity of C20:0 signals on increasing from 4 to 5 mol of C20:0/BSA (Fig. 2H), suggesting saturation of binding sites for C20:0 at 4 to 5 mol.

The signals of the carboxyl of C20:0 appear to be slightly narrower than those in the spectra of oleic acid. Close examination suggests that this reflects more homogeneous signals for C20:0, possibly because of a lower conformational variability of BSA, or decreased occupancy of

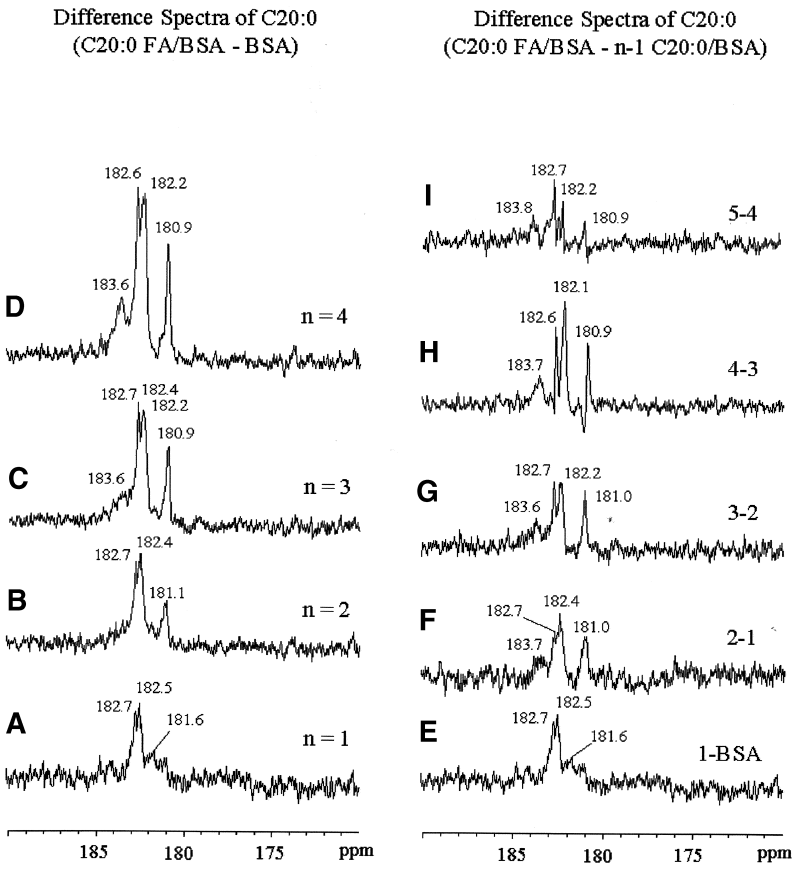

Fig. 2. Carboxyl and carbonyl region (170–190 ppm) of the ^{13}C-NMR spectra of arachidic acid (C20:0) bound to BSA between 1 and 4 mol C20:0/mol BSA after 2,400 spectral accumulations. A–D: The contribution of BSA was subtracted digitally. E–I: Difference spectra of (N+1) C20:0/BSA–N C20:0/BSA. All spectra were acquired as in Fig. 1.

lower affinity sites available to oleic acid. The narrow peaks for C20:0 and the other VLCFA indicate that the carboxyl group is mobile within the binding sites and is not more significantly restricted than that for long-chain fatty acids.

Extension of the acyl chain by two carbons to C22:0 results in changes in binding properties, as observed by ^{13}C-NMR spectroscopy. The most prominent signal at 1 and 2 mol C22:0/BSA (182.6–182.7 ppm) increases in intensity up to 3 mol C22:0/BSA and then ceases to increase (**Fig. 3**). By comparison, a peak at this chemical shift appeared in the spectra of C20:0 at low mol ratios but did not saturate until 4 mol C20:0/BSA. For oleic acid, a peak at this position represented only a minor low-affinity site. The relative intensity of the signal at 181 ppm, which is relatively weak for C20:0 at 1:1 mol ratio (Fig. 2B) compared with that for oleic acid (Fig. 1B), is further reduced in intensity for C22:0 at 1:1 and 2:1 ratios (Fig. 3A, B). At 3:1 and 4:1 ratios of C22:0-BSA, NMR spectra reveal three to four different signals (with similar intensities), at chemical shifts very similar to those for C20:0. The main peaks showing an increase in intensity between 3 and 4 mol (181.1 and 182.1 ppm) are the same for C22:0 as for C20:0. The difference spectra show constant increases in intensity with each mol of C22:0, although these increases are smaller than those observed for the shorter-chain fatty acids. These results may reflect precipitation of some of the C22:0 with each addition to BSA, even though our method of incremental additions of VLCFA was designed to minimize precipitation (see Materials and Methods). There is a small increase in intensity between 3 and 4 mol and no measurable increase in intensity in any peaks after the addition of the fifth mol of C22:0. This suggests that the binding of C22:0 to BSA reaches saturation with 3 to 4 mol of fatty acid/BSA.

Transfer of C22:0, C24:0, and C26:0 from vesicles to BSA

Since the solubility of C24:0 is too low to permit delivery of VLCFA to BSA directly as the potassium salt, SUV were used as vehicles to deliver VLCFA indirectly via the partitioning of VLCFA from vesicles to BSA. Low proportions of C24:0 were incorporated into SUV by co-sonication with PC (see Materials and Methods), and fatty acid-free BSA was mixed with an equal volume of this suspension. Because previous fluorescence studies indicated that the rate of desorption of C24:0 from phospholipid vesicles is slow (28) ($t_{1/2}$ = ~30 min), spectra were obtained as a function of time.

Spectra of the carbonyl region of the PC vesicles with 5.5 mol% of C24:0 are presented in **Fig. 4A**. The intense, narrow resonance at 178.3 ppm represents VLCFA incorporated in the SUV; the extremely low concentration of unbound fatty acid would not give an observable signal, as also in the case of VLCFA/BSA complexes. The two reso-

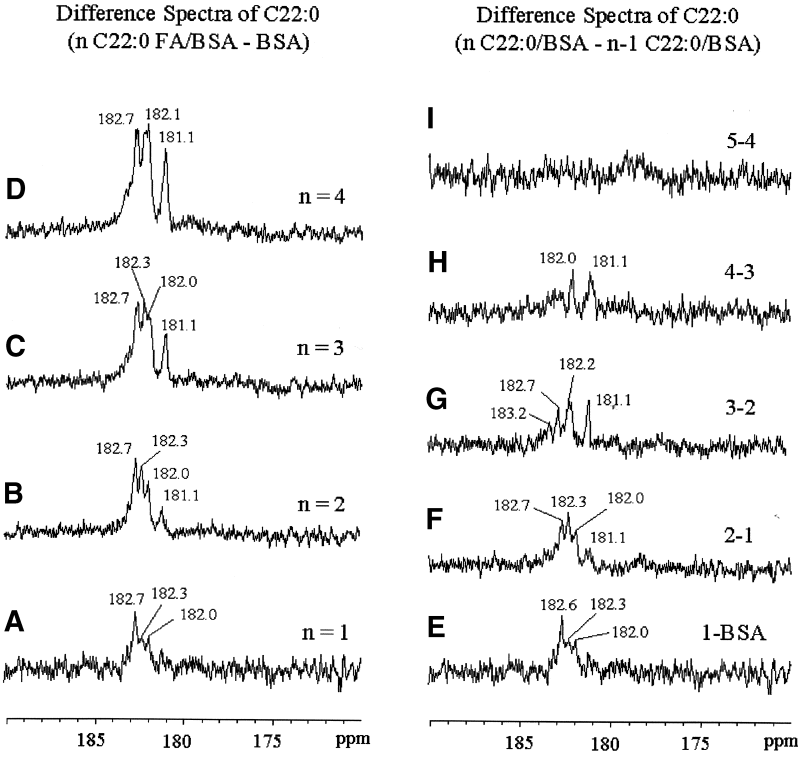

Fig. 3. Carboxyl and carbonyl region (170–190 ppm) of the ^{13}C-NMR spectra of behenic acid (C22:0) bound to BSA between 1 and 4 mol C22:0/mol BSA after 2,400 spectral accumulations. A–D: The contribution of BSA was subtracted digitally. E–I: Difference spectra of N C22:0/BSA–N-1 C22:0/BSA. All spectra were acquired as in Fig. 1.

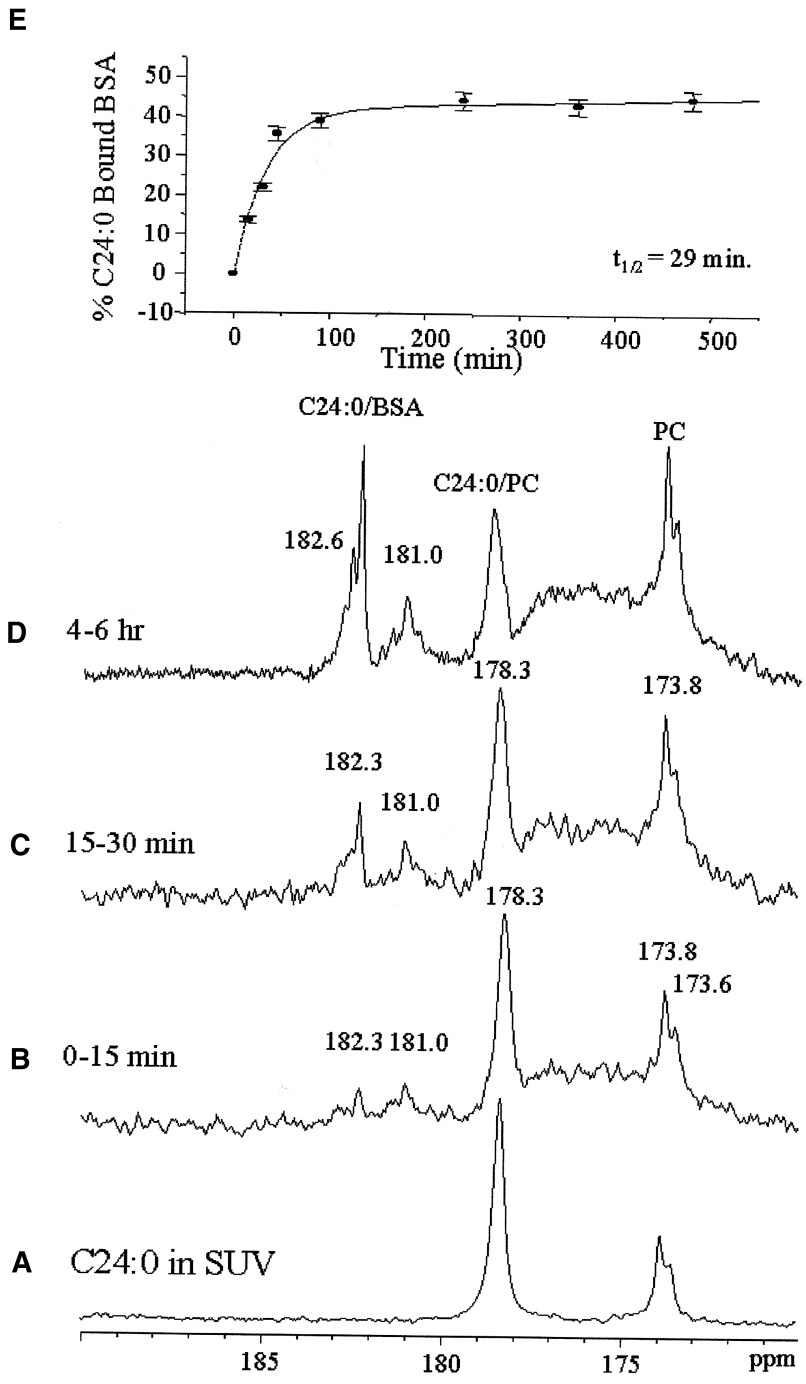

Fig. 4. Carboxyl and carbonyl regions (170–190 ppm) of ^{13}C-NMR spectra. [1-^{13}C]lignoceric acid (C24:0) was cosonicated with egg phosphatidylcholine (PC) to prepare small unilamellar vesicles (SUV) containing very long-chain fatty acids. The intense peak at 178.2 ppm (A) is from the carboxyl carbon of C24:0 bound to SUV. The intensity of this peak decreased with time due to the transfer of C24:0 from SUV to BSA. BSA was added to the SUV complex at the time point 0. The two peaks at 173.8 and 173.6 ppm are from phospholipid carbonyls, and their intensities do not vary with time. All samples were acquired at 35°C with a pulse interval 2.0 s and 32,000 time-domain points. Spectra A and D were acquired after 2,400 spectral accumulation with line broadening of 10 Hz and 5 Hz, respectively. Spectra B and C were acquired after 300 scans with line broadening of 10 Hz. The vertical scales were adjusted to make the peak intensities of the phospholipid carbonyls approximately equal. E: The plot of normalized intensity of the signal of C24:0 bound to BSA versus time. The percentage of C24:0 transferred from SUV to BSA was determined by the area of the peak for C24:0 bound to BSA divided by the sum of the peak areas of the C24:0 bound to BSA and the peak representing C24:0 bound to SUV. The data points were fit to a first-order exponential function.

nances at 173.6 and 173.8 ppm are from the carboxyl group of PC in the inner and outer leaflets, respectively, of the SUV; their intensities did not change throughout the experiment, reflecting the constant amount of PC. After the addition of BSA to the SUV (Fig. 4B), a new signal at 181.0 ppm from protein glutamic acid carboxyls (Fig. 1A) became evident immediately but remained relatively unchanged over time. Another new signal at 182.3 ppm became detectable in the first (0–15 min) time interval (Fig. 4B). Spectra were then obtained in 15 min time blocks to permit the transfer process to be observed while maintaining sufficient signal-to-noise ratios (selected spectra are shown in Fig. 4B, C). Over time, the signal at 182.3 ppm grew steadily until it reached equilibrium (Fig. 4D). A second smaller peak at 182.6 ppm was observed at 45 to 60 min. The peak at ~181.0 ppm seen for all shorter-chain fatty acids was very weak (if present at all) for C24:0.

The fraction of VLCFA (C24:0) bound to BSA is plotted as a function of time in Fig. 4E. The data were well fitted by a first-order exponential transfer function, from which a half time ($t_{1/2}$) of 29 min was calculated. For C24:0 transfer experiments, we used two different concentrations of C24:0 in vesicles, corresponding to stoichiometric ratios of 1.2 mol C24:0/BSA (data not shown) and 3.1 mol C24:0/BSA (Fig. 4). In the latter experiment, we estimate that 1.5 mol of C24:0 was bound to BSA, on the basis of the relative intensities of C24:0 peaks representing binding to albumin and vesicles. Both experiments showed the same two binding sites on BSA (182.3 and 182.6 ppm). The $t_{1/2}$ for transfer was the same for the lower ratio.

To validate this approach for determining binding sites for C24:0 on BSA, we applied the same approach to C22:0, for which we have data from direct addition of C22:0 to BSA. C22:0 was incorporated into SUV, and fatty acid-free BSA was then added to achieve 3.6 mol of C22:0/mol of BSA. Spectra (**Fig. 5**) showed three prominent peaks at the same chemical shifts as those seen with the direct binding studies at 2 mol of C22:0/BSA, which is below the saturation of C22:0 binding to the protein (Fig. 3B).

We previously studied binding of C26:0 to BSA by the same strategy as described above for C24:0 (26). We repeated experiments with C26:0 prepared to a higher degree of purity (see Materials and Methods). Transfer experiments (not shown) revealed slow transfer ($t_{1/2}$ ~1.6 h at 38°C), a single binding site at 182.7 ppm, and maximal binding of 1 mol of C26:0, in agreement with the determinations of Ho et al. (26).

Competition of C18:1 and C22:0 for binding sites on BSA

We carried out a competition experiment to determine whether VLCFA bind to BSA in the presence of a typical long chain fatty acid. **Fig. 6** shows spectra of ^{13}C-labeled C22:0 in the presence of unlabeled oleic acid. Oleic acid was chosen because it is the most abundant fatty acid in the plasma and has the highest affinity for albumin of any dietary fatty acid, as measured by classical affinity-constant determinations (5, 29). At the levels of oleic acid added, its carboxyl signal is not detected and the spectra reflect only the VLCFA carboxyl. The spectrum of C22:0 alone (Fig. 6A) shows three distinct binding environments when 2 mol of VLCFA are present. (Note that the protein component was not subtracted as in Fig. 2, and is the major contribution to the peak at 181.0 ppm.) The first addition of oleic acid (**Fig. 7B**) results in a loss of intensity of the peak at 182.2 ppm, and this peak is completely absent with >3 mol of oleic acid (Fig. 7C–E). At the same time, a new signal at 183.4 ppm is first seen with 2 mol of oleic acid (Fig. 7B) and grows in intensity with increasing amounts of oleic acid. The site at 182.2 ppm is the chemical shift for one of the primary binding sites of oleic acid (Fig. 1). A peak at 183.5 ppm has been observed previously for oleic acid and other long-chain fatty acids; it is first detected as a weak signal with 3 mol of oleic acid (Fig. 1D) and increases to a maximum intensity at 5 mol (10). Therefore, in the presence of oleic acid, C22:0 can be dis-

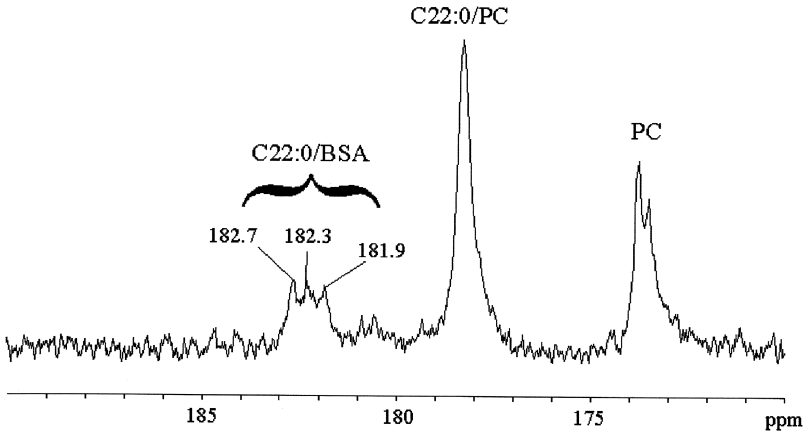

Fig. 5. Transfer of C22:0 from SUV to BSA. Carboxyl and carbonyl region (170–190 ppm) of ^{13}C-NMR spectra of C22:0 bound to SUV and BSA after reaching the equilibrium. BSA in solution was added to the SUV containing C22:0. The contribution of BSA was removed by subtracting the BSA spectrum. The figure shows multiple binding sites of C22:0 on BSA and an intense peak from C22:0 bound to SUV. The spectrum was processed with 3 Hz line broadening after 2,400 scans.

placed from a primary binding site for oleic acid into this medium-affinity site.

In the competition experiment, the peak at 182.6 to 182.7 ppm is not affected by the addition of oleic acid until a high ratio is reached (5 mol of oleic acid; 7 mol of total fatty acid). This signal is observed consistently with all VLCFA and is the only peak for C26:0. A peak at the same position is seen as a very weak shoulder in spectra of oleic acid (Fig. 1) and was detected previously for oleic acid only at mol ratios of fatty acid-BSA >6 (10). This medium- or low-affinity site for long-chain fatty acids is probably identical to the high-affinity site for VLCFA. The peak for C22:0 at 181.9–182.0 ppm is also not affected by the addition of oleic acid. This chemical shift, however, is very close to that for one of the three highest-affinity sites for oleic acid. It is not clear whether this is the same binding site for both fatty acids, and the affinity of C22:0 is greater for this site, or is a different site for C22:0 and oleic acid, with a very similar local environment for the two fatty acids.

DISCUSSION

In our investigation of the binding of VLCFA to albumin, we used approaches similar to those developed for medium- and long-chain fatty acids. Previous studies of saturated fatty acids (8–18 carbons) with increasing fatty acid-BSA ratios revealed distinct binding sites and the dis-

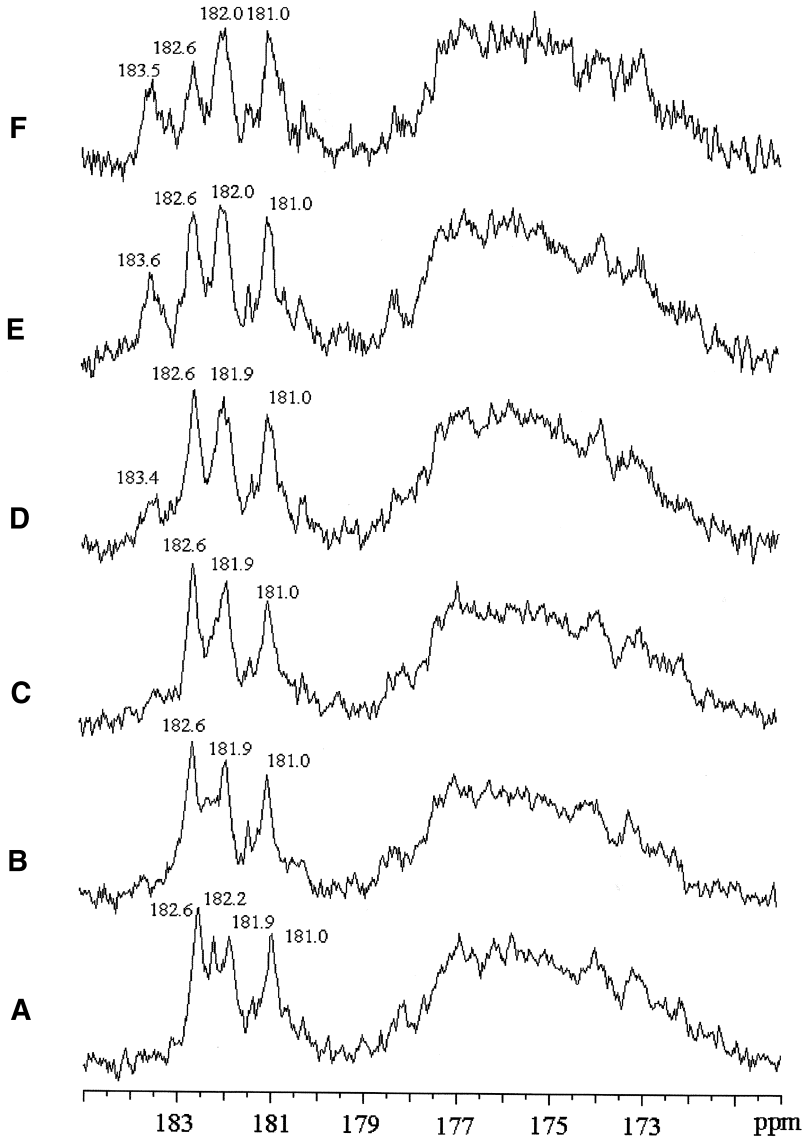

Fig. 6. Competition between C18:1 and C22:0. Carboxyl and carbonyl region of ^{13}C-NMR spectra of the competition between [1-^{13}C]C22:0 and naturally abundant oleic acid for binding sites on BSA. Increments of oleate from 1 mol to 5 mol were added to 2 mol [1-^{13}C]C22:0/BSA. A: 2 mol [1-^{13}C]C22:0/BSA. B–F: 1 to 5 mol C18:1 + 2 mol [1-^{13}C]C22:0/BSA. The spectra were acquired after 2,400 accumulation at 35°C with a 2.0 s pulse interval.

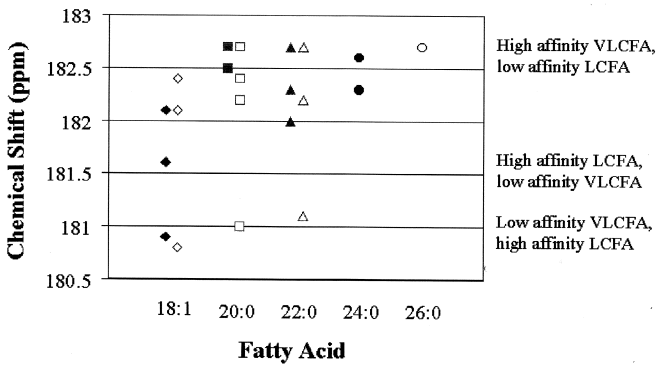

Fig. 7. Summary of binding sites on BSA for oleic acid and very long-chain fatty acids (C20:0, C22:0) from direct binding studies at two different mol ratios (1 and 3 mol fatty acid/BSA) and for C24:0 and C26:0 from partitioning experiments. Symbols are: 1 mol C18:1/BSA (closed diamond); 3 mol C18:1/BSA (open diamond); 1 mol C20:0/BSA (closed square); 3 mol C20:0/BSA (open square); 1 mol C22:0/BSA (closed triangle); 3 mol C22:0/BSA (open triangle); ~1 mol C26:0/BSA (open circle). Our assignments of peaks to high and low affinity binding sites (on the basis of filling of individual sites) are shown.

tribution of fatty acids in these sites. The spectra of long-chain fatty acids showed up to seven carboxyl peaks; three peaks predominated at ≤3 mol fatty acid/BSA (high-affinity sites), and additional peaks appeared at ≥3 mol fatty acid/BSA (medium- and low-affinity sites). More recently, the crystal structure of albumin with saturated fatty acids with eight to 18 carbons has located seven binding sites for fatty acids with 12 to 18 carbons (15). Five of the seven sites are stabilized by close interactions of the fatty acid carboxyl group with basic amino acids, and the positioning of the carboxyl in these sites is essentially identical for all fatty acid chain lengths. The X-ray structure thus supports our previous hypothesis that each distinct carboxyl peak represents a unique binding site. Furthermore, we can postulate that the chemical shift of the bound fatty acid is independent of chain length up to 18 carbons for most binding sites, so that the same chemical shift represents the same site for different long-chain fatty acids. As discussed below, this postulate can be extrapolated (cautiously) to VLCFA.

Figure 7 summarizes chemical shift data for oleic acid and VLCFA at selected fatty acid/BSA mole ratios. For VLCFA we observed carboxyl peaks at the same chemical shifts seen for long-chain fatty acids, but the relative intensities changed differently with increasing mol ratios of VLCFA, reflecting different relative affinities of the binding sites. The highest-affinity sites for C20:0 corresponded to peaks at 182.5 and 182.7 ppm, and the high-affinity site at 181.0 ppm for oleic acid was not seen at 1 mol of C20:0. Above 4 mol C20:0/BSA, binding was almost completely saturated. The spectra of C22:0 revealed binding sites with about the same chemical shifts as for C20:0. The highest-affinity binding sites corresponded to the peak at 182.7 ppm; this peak and the two additional high-affinity sites (182.3 and 182.0 ppm) showed saturation above 3 mol C22:0/BSA, but the lower affinity site at 181.1 ppm continued to increase up to 4 mol. The partitioning of C24:0 from SUV to BSA revealed at least two sites on BSA. In addition, both our present and our previous study (26) showed one carboxyl resonance (182.7 ppm) for C26:0.

The occupancy of the site represented by the peak at 181.1 ppm decreases with chain length. Whereas this is a high-affinity site for long-chain fatty acids (and is an intense signal at the lowest ratios of oleic acid), this peak is first seen (as a weak signal) with 2 mol of C20:0 and is barely detected with 3 mol of C22:0. For both these VLCFA, the intensity increases to a level that suggests binding of a total of 1 mol. However, occupancy of this site is insignificant for C24:0 and C26:0. The binding site represented by this peak has been localized to domain 1 in the structure of albumin by studies of oleic acid binding to fragments of BSA (30), and most likely is similar to binding site 1 or 2 in the crystal structure of HSA (16, 17).

As this site becomes less significant for VLCFA, a site corresponding to 182.6 to182.7 ppm becomes increasingly significant and is the only site for C26:0. Because this peak is well separated from the peak at 181 ppm, we postulate that these are different binding sites and not the same site altered drastically by chain length-dependent interactions. Furthermore, in competition studies the peak at 182.7 ppm for C22:0 is not affected by up to 4 mol of oleic acid. A peak at 182.6 ppm appears at high mol ratios of fatty acid-BSA for long-chain fatty acids such as oleic acid (10). Therefore, this is either a low-affinity site for long-chain fatty acids that is preferred by VLCFA or a unique site for VLCFA; the latter possibility is considered less likely.

C20:0 and C22:0 also show multiple peaks in the range of 182.0 to182.5 ppm, where peaks corresponding to high- and medium-affinity sites for long-chain fatty acids are seen. The results of competition studies between oleic acid and C22:0 strongly imply that one of these sites is a high-affinity site for oleic acid (182.2 ppm).

Binding affinities for saturated fatty acids increase with increasing chain length up to C18:0 (5), but the affinity constant for C20:0 suggested diminished binding for this VLCFA (5). We cannot derive affinity constants from our NMR data, but our data show that the number of binding sites and the capacity for binding decreases with increasing chain length after 20 carbons. The maximum capacity of BSA for VLCFA decreases with increasing chain length. The binding of C20:0 saturates with 4 to 5 mol; C22:0, with 3 to 4 mol; C24:0, with 2 mol; and C26:0, with 1 mol. With this trend, we predict that binding of VLCFA with chain lengths longer than 26 to BSA will be very weak.

Reduced binding of VLCFA to albumin could be caused by the inability of the longer chains to fit into binding pockets designed for typical dietary fatty acids. The main stabilizing forces for binding of fatty acids come from *i*) the hydrophobic interactions between the alkyl chain of fatty acids and hydrophobic amino acids of albumin, and *ii*) the electrostatic interaction between the carboxylate group of fatty acids and positively charged residues located at or near the surface of the channel (10, 31). For typical dietary fatty acids, hydrophobic interactions are

considered to constitute most of the binding energy (5). The length of VLCFA is from 25.4 Å (for C20:0) to 33.0 Å (for C26:0) based on 1.27 Å per methylene group (32). If the fatty acid is longer than the binding channel, alterations in the carboxyl region might weaken electrostatic interactions or hydrophobic interactions of the tail of fatty acids might be diminished.

Of the seven binding sites for long-chain fatty acids in the crystal structure of HSA, five sites show limitations in the length of the hydrophobic pocket (15). Site 1 is relatively open and accessible to water and has relatively weak electron density for stearic acid (18:0) compared with shorter-chain fatty acids, suggesting lower occupancy at this site. For fatty acids with >14 carbons, the hydrocarbon tail must curl in the binding site. In site 2, the methyl group of C18:0 is located at the aqueous interface of the channel. In site 3, fatty acids with >14 carbons are forced to make a U-shaped bend. In sites 4 and 5, the methyl group of C18:0 extends into the water at one end of the channel. It is most likely that the binding of longer chains is limited by unfavorable free energy caused by exposure of hydrocarbons to water or by drastic bends in the chain.

Modeling C26:0 into the structure of HSA supports this hypothesis (**Fig. 8**). In four of the sites (numbered 1, 2, 4, and 5), C26:0 is predicted to protrude from the pocket by six or seven methylene units. This portion of the fatty acid would therefore not contribute to the binding energy. It was also evident (data not shown) that site 3, which lies in subdomain IIIA and is closed at the end distal to the carboxylate group, is not large enough to accommodate a molecule of C26:0. As concluded also from our analysis of chemical shifts, the single site for C26:0 probably is a low affinity site for long-chain fatty acid. The modeling exercise strongly suggests that limitations of the binding of VLCFA as seen in our study result from the characteristics of the binding sites of albumin rather than from experimental limitations in solubilizing and manipulating VLCFA.

From the binding competition studies (Fig. 6), we conclude that oleic acid displaces C22:0 from one of its primary binding sites into another binding site (183.5 ppm) that is a medium-affinity site for oleic acid. However, there is remarkably little net displacement of C22:0 from BSA. This suggests that under usual conditions in the plasma, where the fatty acid/albumin ratio is <3, the binding of common dietary fatty acids would not interfere with the binding of VLCFA, which are normally much less abundant.

The amount of saturated VLCFA (C20:0–C26:0) in plasma (esterified and non-esterified) constitutes about 3.1% of total fatty acids for normal humans and 4.8% of the total for patients with adrenoleukodystrophy or adrenomyeloneuropathy (24). To our knowledge, the quantitation of both unesterified and esterified VLCFA in the plasma of such patients has not been reported. Comparison of data from different studies suggests that about 50% of C26:0 could be present in plasma in the unesterified form (H. Moser, personal communication). In light of our new results, we have modified our previous hypothesis that ineffective binding of VLCFA by albumin will limit the removal of VLCFA from cells (26). Because of the low concentrations of VLCFA and the presence of one or more binding sites on albumin, such a limitation is not likely for VLCFA up to and including 26 carbons. Moreover, the VLCFA studied (20–26 carbons) appear to have a preferred binding site on BSA (182.6–182.7 ppm), which could permit their binding even in the presence of much higher concentrations of long chain fatty acids. However, extrapolation of our binding data suggests that binding of longer-chain VLCFA to albumin will be negligible. The delivery of such fatty acids to cells as well as their potential removal from cells would probably be dependent on

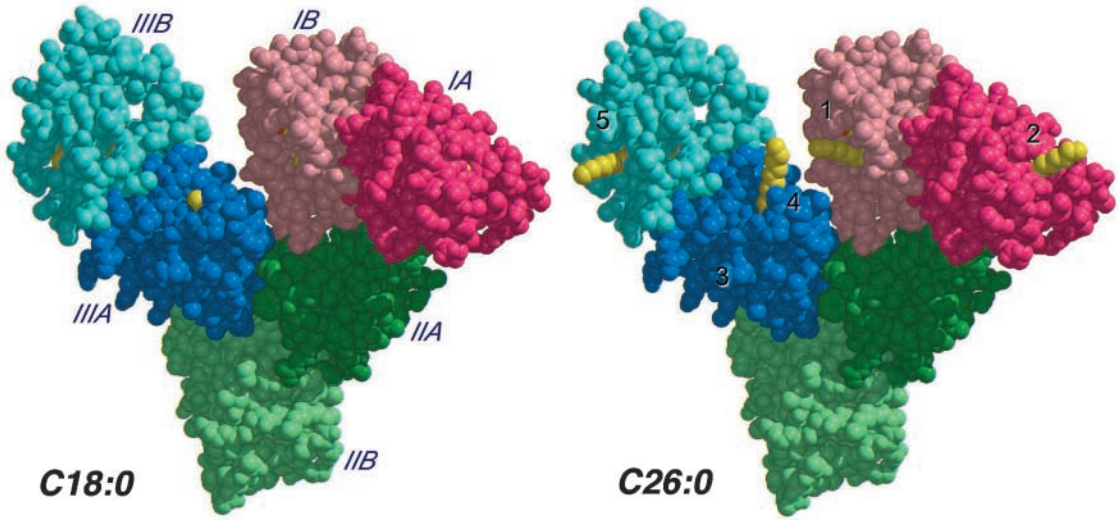

Fig. 8. Structure of HSA with C18:0 (left panel) and C26:0 modeled into the presumed highest affinity binding sites for long chain fatty acids (right panel). Binding sites 1–5 are labeled in the right panel; C18:0 is present in site 3 but not visible. The three domains (I–III) and the two subdomains of each domain (A, B) of albumin are labeled in the left panel. The methylene tail (yellow) of C26:0 protrudes into the water in four of the sites, and site 3 is not large enough to accommodate the C26:0 (see Discussion) This figure was prepared with Raster3D (34) and Bobscript (35).

plasma lipoproteins, and their metabolic fate in cells could be different from that of fatty acids delivered by albumin. In studies of the partitioning of saturated fatty acids with 16 to 24 carbons between human albumin and plasma lipoproteins, partitioning to lipoproteins began with a chain length of 18 carbons, and was favored by increasing chain length (33). Unlike albumin, there is not likely to be a strict limit on the chain length that can bind to lipoproteins. On the basis of this previous study and our new study, it is imperative that whole plasma must be analyzed to quantitate plasma VLCFA rather than the albumin fraction, which is sufficient for typical long chain dietary fatty acids.

This work was supported by National Institutes of Health Grant HL26335 to J.A.H. and HL16660 to R.B. and funding by the BBSRC to S.C. The authors thank Dr. Hugo Moser for helpful comments.

REFERENCES

1. Brown, J. R., and P. Shockley. 1982. Serum albumin: strucure and characterization of its ligand binding sites. *In* Lipid Protein Interactions. P. Jost and O. H. Griffith, editors. John Wiley & Sons, New York. 25–68.
2. Foster, J. F. 1977. Some aspects of the structure and conformational properties of serum albumin. *In* Albumin: Structure, Function, and Uses. V. M. Rosenoer, M. Oratz, and M. A. Rothschild, editors. Pergamon Press, New York. 53–84.
3. Peters, T., and R. G. Reed. 1978. Serum albumin conformation and active sites. *In* 11th FEBS Meeting. T. Peters and I. Sjoholm, editors. Pergamon Press, Copenhagen. 11–20.
4. Peters, T., Jr. 1995. All About Albumin: Biochemistry, Genetics, and Medical Applications. Academic Press, San Diego, CA.
5. Spector, A. A. 1975. Fatty acid binding to plasma albumin. *J. Lipid Res.* **16:** 165–179.
6. Spector, A. A., and J. C. Hoak. 1969. An improved method for the addition of long-chain fatty acid to protein solutions. *Anal. Biochem.* **32:** 297–302.
7. Cistola, D. P., M. T. Walsh, R. P. Corey, J. A. Hamilton, and P. Brecher. 1988. Interactions of oleic acid with liver fatty acid binding protein: a carbon-13 NMR study. *Biochemistry.* **27:** 711–717.
8. Cistola, D. P., J. C. Sacchettini, L. J. Banaszak, M. T. Walsh, and J. I. Gordon. 1989. Fatty acid interactions with rat intestinal and liver fatty acid-binding proteins expressed in *Escherichia coli*. *J. Biol. Chem.* **264:** 2700–2710.
9. Cistola, D. P., J. C. Sacchettini, and J. I. Gordon. 1990. ^{13}C NMR studies of fatty acid-protein interactions: comparison of homologous fatty acid-binding proteins produced in the intestinal epithelium. *Mol. Cell. Biochem.* **98:** 101–110.
10. Parks, J. S., D. P. Cistola, D. M. Small, and J. A. Hamilton. 1983. Interactions of the carboxyl group of oleic acid with bovine serum albumin: a ^{13}C NMR study. *J. Biol. Chem.* **258:** 9262–9269.
11. Cistola, D. P., D. M. Small, and J. A. Hamilton. 1987. Carbon 13 NMR studies of saturated fatty acids bound to bovine serum albumin. I. Electrostatic interactions in individual fatty acid binding sites. *J. Biol. Chem.* **262:** 10980–10985.
12. Cistola, D. P., D. M. Small, and J. A. Hamilton. 1987. Carbon 13 NMR studies of saturated fatty acids bound to bovine serum albumin. II. The filling of individual fatty acid binding sites. *J. Biol. Chem.* **262:** 10971–10979.
13. Hamilton, J. A., D. P. Cistola, J. D. Morrisett, J. T. Sparrow, and D. M. Small. 1984. Interactions of the carboxyl group of oleic acid with bovine serum albumin; a ^{13}C NMR study. *Proc. Natl. Acad. Sci. USA.* **81:** 3718–3722.
14. Hamilton, J. A. 1992. Binding of fatty acids to albumin: a case study of lipid-protein interactions. *News Physiol. Sci.* **7:** 264–270.
15. Bhattacharya, A. A., T. Grune, and S. Curry. 2000. Crystallographic analysis reveals common modes of binding of medium- and long-chain fatty acids to human serum albumin. *J. Mol. Biol.* **303:** 721–732.
16. Curry, S., H. Mandelkow, P. Brick, and N. Franks. 1998. Crystal structure of human serum albumin complexed with fatty acid reveals an asymmetric distribution of binding sites. *Nat. Struct. Biol.* **5:** 827–835.
17. Curry, S., P. Brick, and N. P. Franks. 1999. New insights from crystallography. *Biochim. Biophys. Acta.* **1441:** 131–140.
18. Moser, H. W., K. D. Smith, and A. B. Moser. 1995. X-linked adrenoleukodystrophy. *In* The Metabolic and Molecular Basis of Inherited Disease. C. R. Scriver, A. L. Beaudet, W. S. Sly, and D. Valle, editors. McGraw Hill, New York. 2325–2349.
19. Hirsch, D., A. Stahl, and H. F. Lodish. 1998. A family of fatty acid transporters conserved from mycobacterium to man. *Proc. Natl. Acad. Sci. USA.* **95:** 8625–8629.
20. Steinberg, S. J., S. J. Wang, M. C. McGuinness, and P. A. Watkins. 1999. Human liver-specific very-long-chain acyl-coenzyme A synthetase cDNA cloning and characterization of a second enzymatically active protein. *Mol. Genet. Metab.* **68:** 32–42.
21. Steinberg, S. J., J. J. Wang, D. G. Kim, S. J. Mihalik, and P. A. Watkins. 1999. Human very-long-chain acyl-CoA synthetase: cloning, topography, and relevance to branched fatty acid metabolism. *Biochem. Biophys. Res. Commun.* **257:** 615–621.
22. Coe, N. R., A. J. Smith, B. I. Frohnert, P. A. Watkins, and D. A. Bernlohr. 1999. *J. Biol. Chem.* **274:** 36300–36304.
23. Brown III, F. R., W. W. Chen, D. A. Kirschner, K. L. Frayer, J. M. Powers, A. B. Moser, and H. W. Moser. 1983. Myelin membrane from adrenoleukodystrophy brain white matter—biochemical properties. *J. Neurochem.* **41:** 341–348.
24. Moser, H. W., A. B. Moser, K. K. Frayer, W. Chen, J. D. Schulman, B. P. O'Neill., and Y. Kishimoto. 1981. Adrenoleukodystrophy: increased plasma content of saturated very long chain fatty acids. *Neurology.* **31:** 1241–1249.
25. Wanders, R. J., R. B. Schutgens, and P. G. Barth. 1995. Peroxisomal disorders: a review. *J. Neuropathol. Exp. Neurol.* **54:** 726–739.
26. Ho, J. K., H. Moser, Y. Kishimoto, and J. A. Hamilton. 1995. Interactions of a very long chain fatty acid with model membranes and serum albumin: implications for the pathogenesis of adrenoleukodystrophy. *J. Clin. Invest.* **96:** 1455–1463.
27. Jones, T. A., J. Y. Zou, S. W. Cowan, and M. Kjeldgaard. 1991. Improved methods for binding protein models in electron density maps and the location of errors in these models. *Acta Crystallogr. A.* **47:** 110–119.
28. Zhang, F., F. Kamp, and J. A. Hamilton. 1996. Dissociation of long and very long chain fatty acids from phospholipid bilayers. *Biochemistry.* **35:** 16055–16060.
29. Goodman, D. S. 1958. The interaction of serum albumin with fatty acid anions. *J. Am. Chem. Soc.* **80:** 3892–3898.
30. Hamilton, J. A., S. Era, S. P. Bhamidipati, and R. G. Reed. 1991. Locations of the three primary binding sites for long-chain fatty acids on bovine serum albumin. *Proc. Natl. Acad. Sci. USA.* **88:** 2051–2054.
31. Swaney, J. B., and I. M. Klotz. 1970. Amino acid sequence adjoining the lone tryptophan of human serum albumin. A binding site for the protein. *Biochemistry.* **9:** 2570–2574.
32. Small, D. M. 1986. The Physical Chemistry of Lipids. Vol. 4. Plenum Press, New York.
33. Shafrir, E., S. Gatt, and S. Khasis. 1965. Partition of fatty acids of 20–24 carbon atoms between serum albumin and lipoproteins. *Biochim. Biophys. Acta.* **98:** 365–371.
34. Merrit, E. A., and D. J. Bacon. 1997. Raster3D: photorealistic molecular graphics. *Methods Enzymol.* **277:** 505–524.
35. Esnouf, R. 1997. An extensively modified version of MolScript that includes greatly enhanced coloring capabilities. *J. Mol. Graph. Model.* **15:** 132–134.